

Z production in pPb collisions at LHCb

Hengne Li^{a,1,*}

^a*Guangdong Provincial Key Laboratory of Nuclear Science, Institute of Quantum Matter, South China Normal University, Guangzhou 510006, China*

E-mail: hengne.li@m.scnu.edu.cn

This article presents results of the Z boson production in the proton-lead collisions at $\sqrt{s_{NN}} = 5.02$ TeV and $\sqrt{s_{NN}} = 8.16$ TeV collected in 2013 and 2016, respectively, by the LHCb detector at the LHC in forward and backward rapidity. The great precision of the 2016 data are found compatible with nPDFs theoretical predictions within large theoretical uncertainties, and can be useful to constraint new predictions.

HardProbes2020
1-6 June 2020
Austin, Texas

¹On behalf of the LHCb collaboration.

*Speaker

The properties of W/Z bosons have been extensively studied at electron-positron and hadron colliders. The production cross-sections of W/Z bosons at hadron colliders can be well described by perturbative Quantum Chromodynamics (pQCD) at next-to-next-to-leading order (NNLO), and the radiative corrections and the input electroweak parameters are also precisely known. The measurements of their production cross-sections in proton-proton (pp) collisions can be used to constrain the initial conditions such as the Parton Distribution Functions (PDFs) of the proton [1, 2].

In the same respect, the production of the W/Z bosons can also precisely probe of the nuclear PDFs, especially the that of heavy quarks and gluon, which are currently less precisely constrained [3]. In proton-ion and ion-ion collisions, the PDFs of nucleons confined in nuclei are found to be different with respect to those of free nucleons, which are called nuclear PDFs (nPDFs) [4–8]. The differences between nPDFs and PDFs are often referred as nuclear modifications, which are understood as a reflection of the various initial state nuclear matter effects on the free nucleons. These effects include the nuclear shadowing [9] appearing as a suppression for Bjorken- x (x in the following, the fraction of a nucleon momentum carried by a parton) below 0.05, the anti-shadowing effect [10, 11] raising the PDFs for x around 0.1, the EMC effect [12] suppressing the PDFs around $0.3 < x < 0.7$, and the fermi motion effect modifies the region for x around 1. The nPDFs are crucial for the studies of the Quark Gluon Plasma (QGP) in the ion-ion collisions, in order to disentangle cold and hot nuclear matter effects.

Moreover, since the W/Z bosons and their leptonic decay products do not participate strong interactions, they inherit perfectly the initial conditions without being modified by the hadronic medium in the intermediate and final states. Therefore, they can be used to better differentiate between properties of the initial- and final-state effects, and the proton-ion collisions provide an ideal environment to study the initial-state nuclear matter effects, hence to constrain the nPDFs.

In this article, we present results of the Z boson production in the proton-lead collisions [13, 14] at the LHC using data collected during 2013 and 2016 by the LHCb detector. The LHCb detector [15, 16] is a fully instrumented single-arm spectrometer in the forward region covering a pseudorapidity acceptance of $2 < \eta < 5$, providing a high tracking momentum resolution down to very low transverse momentum (p_T) and precise vertex reconstruction capability. The proton-lead datasets with their recorded integrated luminosities are given in Table 1.

$\sqrt{s_{NN}}$	2013		2016	
	5.02 TeV		8.16 TeV	
	pPb	Pbp	pPb	Pbp
\mathcal{L}	1.1 nb^{-1}	0.5 nb^{-1}	13.6 nb^{-1}	20.8 nb^{-1}

Table 1: Summary of the LHCb pPb datasets and the recorded integrated luminosities.

The Z boson production cross-sections in the dimuon decay channel are measured in the fiducial volume in both the forward (pPb) and backward (Pbp) collision configurations [13, 14] based on the following equation: $\sigma_{Z \rightarrow \mu^+ \mu^-} = [N_{\text{cand}} \cdot \rho] / [\mathcal{L} \cdot \epsilon]$, where $\sigma_{Z \rightarrow \mu^+ \mu^-}$ is the production cross-section to be measured, N_{cand} is the number of $Z \rightarrow \mu^+ \mu^-$ candidates passing signal selection, ρ is the signal purity of the selected Z candidates, \mathcal{L} is the integrated luminosity, and ϵ is the total efficiency including trigger, reconstruction and selection efficiencies. The fiducial volume is defined as $60 < m_{\mu^+ \mu^-} < 120 \text{ GeV}$, $2.0 < \eta_{\mu^\pm} < 4.5$, and $p_T^{\mu^\pm} > 20 \text{ GeV}$. The purity is measured

using data-driven methods, and the efficiencies are estimated using Monte-Carlo (MC) samples together with tag-and-probe data driven corrections.

The invariant mass distributions of selected signal candidates are shown in Fig. 1 for datasets taken in 2016 at $\sqrt{s_{\text{NN}}} = 8.16$ TeV.

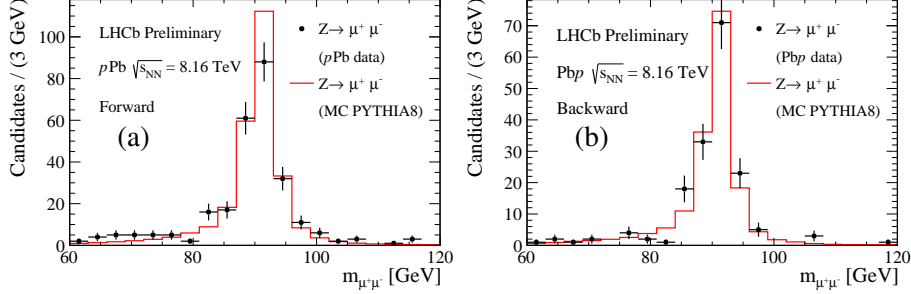


Figure 1: (color online) The dimuon invariant mass distributions after the offline selection for pPb (a) and Pbp (b) configurations, using datasets taken in 2016 at $\sqrt{s_{\text{NN}}} = 8.16$ TeV. The red line shows the distributions from simulation generated using PYTHIA 8 [17] with CTEQ6L1 [18] PDF set, normalised to the number of observed candidates.

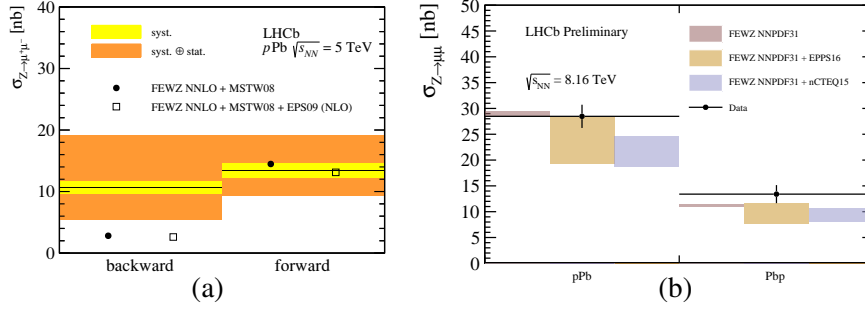


Figure 2: (color online) Measured fiducial cross-sections of Z production and theoretical calculations using various PDF sets with or without nuclear modification. Figure (a) is for dataset taken in 2013 at $\sqrt{s_{\text{NN}}} = 5.02$ TeV and figure (b) is for dataset taken in 2016 at $\sqrt{s_{\text{NN}}} = 8.16$ TeV.

The resulting fiducial cross-sections for centre-of-mass energies at $\sqrt{s_{\text{NN}}} = 5.02$ TeV and 8.16 TeV [13, 14] are shown in Fig. 2 (a) and (b), respectively. The results are compared with theoretical calculations using FEWZ [19, 20] with MSTW08 [21] free nucleon PDF together with EPS09 (NLO) [22] nPDF for dataset at 5.02 TeV, and with NNPDF 3.1 [23] free nucleon PDF together EPPS16 (NLO) [4] and nCTEQ15 (NLO) [3, 24] nPDFs for dataset at 8.16 TeV. The measured cross-section central value is higher than the nPDFs predicted values but in agreement with the theoretical prediction statistically. The results are also compared with previous 5.02 TeV results from LHCb [13], ATLAS [25], CMS [26], and ALICE [27], as shown in Fig. 3. The new LHCb 8.16 TeV results are compatible with previous 5.02 TeV results, but with about 20 times higher statistics. The great precision of these measurements at forward and backward rapidities are able to provide strong constraint, specially at backward rapidity.

The ratio of the Z boson production cross-sections for forward and backward configurations (R_{FB}), is particularly sensitive to cold nuclear effects. R_{FB} is measured in the common rapidity region ($2.5 < |y^*| < 4.0$) in the centre-of-mass frame of the produced Z boson using 2016

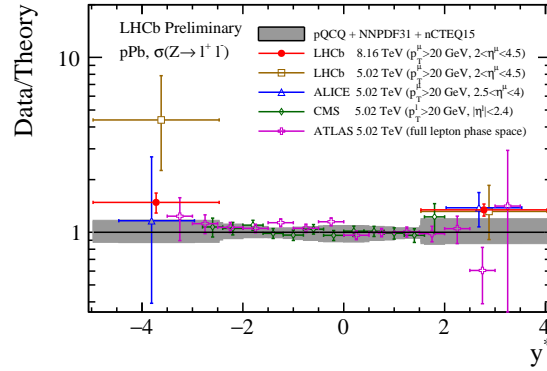


Figure 3: (color online) Comparison of LHCb 8.16 TeV results with previous 5.02 TeV results from ATLAS, CMS, ALICE, and LHCb. The uncertainties on the data over theory ratios include only the experimental statistical and systematic uncertainties; the PDF uncertainties are shown separately on the line at one by the grey band. The central values of the LHCb and ALICE results at 5.02 TeV are shifted to left and right by 0.1 units in rapidity, respectively, for better visibility.

dataset [14] as $R_{\text{FB}}^{2.5 < |y^*| < 4.0} = 1.28 \pm 0.14(\text{stat}) \pm 0.14(\text{syst}) \pm 0.05(\text{lumi})$, which is compatible with theoretical calculations using FEWZ with the following nPDFs: $R_{\text{FB,NNPDF3.1+EPPS16}}^{2.5 < |y^*| < 4.0} = 1.45 \pm 0.10(\text{theo.}) \pm 0.01(\text{num.}) \pm 0.27(\text{nPDF})$, and $R_{\text{FB,NNPDF3.1+nCTEQ15}}^{2.5 < |y^*| < 4.0} = 1.44 \pm 0.10(\text{theo.}) \pm 0.01(\text{num.}) \pm 0.20(\text{nPDF})$, where, the uncertainty “num.” is from the numerical precision.

In summary, LHCb provides an excellent opportunity to probe the cold nuclear matter effects in the very forward region using Z boson production. Results of pPb collisions at 5.02 TeV and 8.16 TeV results are presented, which are compatible with theoretical predictions involving nPDFs, where the 8.16 TeV results give the highest precision in the forward region at LHC, thus can be useful in constraining the current nPDFs.

Acknowledgments

We acknowledge the support from Science and Technology Program of Guangzhou (No. 2019050001).

References

- [1] J. Rojo, et al., The PDF4LHC report on PDFs and LHC data: Results from Run I and preparation for Run II, J. Phys. G42 (2015) 103103. [arXiv:1507.00556](https://arxiv.org/abs/1507.00556), [doi:10.1088/0954-3899/42/10/103103](https://doi.org/10.1088/0954-3899/42/10/103103).
- [2] J. Butterworth, et al., PDF4LHC recommendations for LHC Run II, J. Phys. G43 (2016) 023001. [arXiv:1510.03865](https://arxiv.org/abs/1510.03865), [doi:10.1088/0954-3899/43/2/023001](https://doi.org/10.1088/0954-3899/43/2/023001).
- [3] A. Kusina, F. Lyonnet, D. B. Clark, E. Godat, T. Jezo, K. Kovarik, F. I. Olness, I. Schienbein, J. Y. Yu, Vector boson production in pPb and PbPb collisions at the LHC and its impact on nCTEQ15 PDFs, Eur. Phys. J. C77 (7) (2017) 488.
- [4] K. J. Eskola, P. Paakkinen, H. Paukkunen, C. A. Salgado, EPPS16: Nuclear parton distributions with LHC data, Eur. Phys. J. C77 (3) (2017) 163. [arXiv:1612.05741](https://arxiv.org/abs/1612.05741), [doi:10.1140/epjc/s10052-017-4725-9](https://doi.org/10.1140/epjc/s10052-017-4725-9).
- [5] D. de Florian, R. Sassot, Nuclear parton distributions at next-to-leading order, Phys. Rev. D69 (2004) 074028. [arXiv:hep-ph/0311227](https://arxiv.org/abs/hep-ph/0311227), [doi:10.1103/PhysRevD.69.074028](https://doi.org/10.1103/PhysRevD.69.074028).

- [6] M. Hirai, S. Kumano, T. H. Nagai, Determination of nuclear parton distribution functions and their uncertainties in next-to-leading order, *Phys. Rev. C* 76 (2007) 065207. [arXiv:0709.3038](#), [doi:10.1103/PhysRevC.76.065207](#).
- [7] S. Atashbar Tehrani, Nuclear parton densities and their uncertainties at the next-to-leading order, *Phys. Rev. C* 86 (2012) 064301. [doi:10.1103/PhysRevC.86.064301](#).
- [8] H. Khanpour, S. Atashbar Tehrani, Global analysis of nuclear parton distribution functions and their uncertainties at next-to-next-to-leading order, *Phys. Rev. D* 93 (1) (2016) 014026. [arXiv:1601.00939](#), [doi:10.1103/PhysRevD.93.014026](#).
- [9] R. Glauber, Cross-sections in deuterium at high-energies, *Phys. Rev.* 100 (1955) 242–248. [doi:10.1103/PhysRev.100.242](#).
- [10] J. Ashman, et al., Measurement of the Ratios of Deep Inelastic Muon - Nucleus Cross-Sections on Various Nuclei Compared to Deuterium, *Phys. Lett. B* 202 (1988) 603–610. [doi:10.1016/0370-2693\(88\)91872-2](#).
- [11] S. J. Brodsky, H. J. Lu, Shadowing and Antishadowing of Nuclear Structure Functions, *Phys. Rev. Lett.* 64 (1990) 1342. [doi:10.1103/PhysRevLett.64.1342](#).
- [12] J. Aubert, et al., The ratio of the nucleon structure functions F_{2n} for iron and deuterium, *Phys. Lett. B* 123 (1983) 275–278. [doi:10.1016/0370-2693\(83\)90437-9](#).
- [13] LHCb Collaboration, Observation of Z production in proton-lead collisions at LHCb, *JHEP* 09 (2014) 030.
- [14] LHCb Collaboration, Measurement of Z production cross-sections in proton-lead collisions at $\sqrt{s_{NN}} = 8.16$ TeV.
- [15] LHCb collaboration, The LHCb detector at the LHC, *JINST* 3 (LHCb-DP-2008-001) (2008) S08005.
- [16] LHCb collaboration, LHCb detector performance, *Int. J. Mod. Phys. A* 30 (2015) 1530022.
- [17] T. Sjöstrand, S. Mrenna, P. Skands, A brief introduction to PYTHIA 8.1, *Comput. Phys. Commun.* 178 (2008) 852–867.
- [18] D. Stump, J. Huston, J. Pumplin, W.-K. Tung, H. L. Lai, S. Kuhlmann, J. F. Owens, Inclusive jet production, parton distributions, and the search for new physics, *JHEP* 10 (2003) 046.
- [19] R. Gavin, Y. Li, F. Petriello, S. Quackenbush, FEWZ 2.0: A code for hadronic Z production at next-to-next-to-leading order, *Comput. Phys. Commun.* 182 (2011) 2388–2403.
- [20] Y. Li, F. Petriello, Combining QCD and electroweak corrections to dilepton production in FEWZ, *Phys. Rev. D* 86 (2012) 094034.
- [21] A. D. Martin, W. J. Stirling, R. S. Thorne, G. Watt, Parton distributions for the LHC, *Eur. Phys. J. C* 63 (2009) 189–285.
- [22] K. J. Eskola, H. Paukkunen, C. A. Salgado, EPS09: A New Generation of NLO and LO Nuclear Parton Distribution Functions, *JHEP* 04 (2009) 065.
- [23] NNPDF collaboration, R. D. Ball, et al., Parton distributions from high-precision collider data, *Eur. Phys. J. C* 77 (10) (2017) 663.
- [24] K. Kovarik, et al., nCTEQ15 - Global analysis of nuclear parton distributions with uncertainties in the CTEQ framework, *Phys. Rev. D* 93 (8) (2016) 085037.
- [25] ATLAS collaboration, Z boson production in p+Pb collisions at $\sqrt{s_{NN}} = 5.02$ TeV measured with the ATLAS detector, *Phys. Rev. C* 92 (4) (2015) 044915.
- [26] CMS collaboration, Study of Z boson production in pPb collisions at $\sqrt{s_{NN}} = 5.02$ TeV, *Phys. Lett. B* 759 (2016) 36–57.
- [27] ALICE collaboration, W and Z boson production in p-Pb collisions at $\sqrt{s_{NN}} = 5.02$ TeV, *JHEP* 02 (2017) 077.